

***Ab Initio* Modelling in Solid State Chemistry**

BOOK OF ABSTRACTS

IMPERIAL



THOMAS YOUNG CENTRE
THE LONDON CENTRE FOR
THE THEORY AND
SIMULATION OF MATERIALS



UNIVERSITÀ
DI TORINO



2023 - 2027
DIPARTIMENTO
DI ECCELLENZA
Ministero dell'Università e della Ricerca




Index

Melih Aktas	01
Multiple Topological Phase Transitions in Polyacene Polymers: Ab initio Parametrized Stacked Su-Schrieffer-Heeger Model	
Pietro Andreozzi	02
Modelling Functionalized Carbon Nanodots and their Optical Properties	
Samira Anker	03
Framework for Predictive Modelling of Grain Boundaries	
Sara Balocco	04
First-principles Study of Perovskite Oxide for Solid Oxide Electrochemical Cells: Effects of Cation Substitution on Oxygen Ion Diffusion in $\text{Sr}_2\text{Fe}_{2-x}\text{Mo}_x\text{O}_{6-\delta}$	
Mohammed El Amine Benmalti	05
Computational Analysis of Energetic and Vibrational Frequencies Properties with Solvatochromic Shifts in Uracil-5Water Complexes Using DFT Methods	
Fatma Benyettou	06
Quantum Chemistry Study of Water: <i>Ab Initio</i> Calculation	
Francesca Capellino	07
Applying Nudged Elastic Band in CRYSTAL: Collinear Proton Transfer Reaction Path Analysis	
Chiara Corapi	08
Modelling the Structural and Opto-electronic Properties of Mechanoluminescent Cu-based Hybrid Coordination Polymers	
Shiyu Deng	09
BaFe_2Se_3 : a Quasi-Unidimensional Non-Centrosymmetric Superconductor	
Lukas Diener	10
Synthesis and Characterization of $\text{Na}_{10}\text{Tt}_2\text{Te}_9$ ($\text{Tt} = \text{Ge}, \text{Sn}$): Sodium Tellurotetrelate with Isolated TtTe_4 -Tetrahedra	
Lukas Dopfer	11
Synthesis and Characterization of Halocuprates(I)	

Tea Frey	12
Evaluating Mechanical Behavior in Organic Molecular Crystals Through Computational Modeling	
Beatrice Garetto	13
Ab Initio Tools for XANES & EXAFS Simulations	
Elisabeth Huf	14
Structural Characterization, Electronic Properties and Space Group Stability of LiBaAs Based on DFT Calculations	
Misha Khalid	15
Thermoelectric Performance of Sb Doped ZnO Thin Films Insights from Density Functional Theory and Boltzmann Transport Calculations	
Dennis Kosobokov	16
Elastic properties of Iron-Sulfur alloys at Extreme Conditions	
Sofia Lerda	17
Shedding Light on Photocatalysis by Cobalt Complexes: a Computational Study	
Igors Mihailovs	18
Second Hyperpolarizability of Organic Solvent Molecules in Vacuum, in Liquid and in Crystal	
Felipe Mondaca	19
Exploring the Electronic Properties of HKUST-1: An Experimental and Computational Study	
Filippo Monti	20
Understanding Structure–Property Relationships in Coordination Polymers with CRYSTAL23	
Georg Nowotny	21
Synthesis and Characterisation of Na_5TrSe_4 ($\text{Tr} = \text{Al}, \text{In}$): Sodium Selenidotrirelates with Isolated TrSe_4 Tetrahedra	
Helmy Pacheco Hernández	22
Modulating Two-Photon Absorption in a Pyrene-based MOF Series: Structure-Property Relationships	
Alexander Platonenko	23
Calculations of d-d Transition Energies of Ni^{2+} in KMgF_3 : Effects of Structure, Pressure and Exact Exchange.	

Gabrielė Rankelytė	24
Impact of the Protein Environment on the Excited States of the Pigments in Photosynthetic Complexes	
Peter Remoto	25
Exploring the Complex Solid-State Landscape of Carbamazepine using Low-Frequency Raman Spectroscopy	
Rostislavs Rostovskis	26
From Hybrid-DFT to Million-Atom MD: Accurate and Scalable qSNAP Potential for Radiation Damage in BaF ₂	
Sounak Sarkar	27
Control of Chemical Bonds and Motif Stereochemistry on Magnetic Superexchange in Coordination Network Based Spintronics	
Shuailong Wang	28
Quantum Chemical Investigation of Multi-Redox States in Organic Conjugated Redox Ladder Type Polymers for Electrochemical Energy Storage Systems	
Alina Zhidkovskaya	29
DFT Modeling Data Curation for Machine Learning Applications	

Publication date: 31/07/2025

This work is licensed under CC BY 4.0 

Multiple Topological Phase Transitions in Polyacene Polymers: Ab initio Parametrized Stacked Su-Schrieffer-Heeger Model

Melih Aktas,^a Mohammadreza Mosaferi,^b Jérôme Saint-Martin,^c Alex W. Chin,^b and Davide Romanin^a

^a*Université Paris-Saclay, CNRS, Centre de Nanosciences et de Nanotechnologies, 91120 Palaiseau, Paris, France*

^b*Sorbonne Université, CNRS, Institut des Nanosciences de Paris, UMR7588, F-75252 Paris, France*

^c*Université Paris-Saclay, ENS Paris-Saclay, CNRS, SATIE, 91190 Gif-sur-Yvette, France*

e-mail: melih.aktas@universite-paris-saclay.fr

Single-bridged polyacene polymers are a promising class of organic one-dimensional semiconductors for optoelectronic and energy-conversion applications due to their strong light absorption, low cost, and tunable bandgap, which can host nontrivial topologically insulating phases, without the need of spin-orbit coupling. Their electronic structure can be modeled via the well-known Su-Schrieffer-Heeger (SSH) model^{1, 2} : by tailoring the monomer size and the chain length, signatures of a topological phase transition such as band parity inversion and the emergence of midgap edge states were captured both theoretically and experimentally.

In this work, by using *ab initio* methods and effective tight-binding Hamiltonians, we show that in their multibridged configuration, it is possible to tune the topological phase of the polyacene polymers by varying the number of bridges and their relative position. Moreover, we show that these multibridged polymers can be described by a stacked SSH model, consisting of two closely separated, aligned and equivalent SSH chains, where interchain hoppings and next-nearest-neighbor interactions play a crucial role in stabilizing a multitude of nontrivial topologically insulating phases. This model can be used to describe any couple of interacting and aligned SSH-like chains³.

As a future direction, we are interested in modeling the electronic transport on these polymers, considering both their crystalline configuration, and the nanojunction geometry. In particular, we are interested to see how the topological midgap edge states contribute to the transport properties.

D.R. and M.A. acknowledge support from the HPC resources of IDRIS, CINES, and TGCC under Allocation No. 2024-A0160914101 made by GENCI, as well as funding from the project TyLDE (Grant No. ANR-23-CE50-0001) founded by the French National Research Agency. A.W.C. and M.M. wish to acknowledge support from the ANR Project ACCEPT (Grant No. ANR-19-CE24-0028).

- [1] B. Cirera, A. Sánchez-Grande, B. dela Torre, et al., Nature Nanotechnology 15:437-443, (2020) Tailoring topological order and π -conjugation to engineer quasi-metallic polymers
- [2] D. Romanin, M. Calandra, A. W. Chin, Phys. Rev. B 106:155122, (2022) Excitonic switching across a \mathbb{Z}_2 topological phase transition: From Mott-Wannier to Frenkel excitons in organic materials
- [3] M. Aktas, M. Mosaferi, J. Saint-Martin, A. W. Chin, D. Romanin, Phys. Rev. B (accepted) Multiple topological phase transitions in double-bridged polyacene polymers: Ab initio parametrized stacked Su-Schrieffer-Heeger model

Modelling functionalized carbon nanodots and their optical properties

Pietro Andreozzi,^a Daniele Perilli^a and Cristiana Di Valentin^a

^a*University of Milano-Bicocca, Department of Materials Science, via Cozzi 55, Milano – ITALY*

e-mail: p.andreozzi@campus.unimib.it

My work of master thesis is devoted to the design and preparation of quantum chemical models of carbon nanodots that highly reproduce the structural properties and functionalization of experimental systems prepared in the group of Prof. Gennara Cavallaro at the University of Palermo [1]. These systems are characterized by high surface area, good photothermal conversion, which can be applied in nanomedicine for therapy and diagnostics. The model shown in Figure 1 represents a spherical nanoparticle of β -C₃N₄ and is functionalized with several groups at the surface that can be used to activate the coating with polymers to improve biocompatibility and stealth properties. The CRYSTAL17 code has been used to fully relax the atomic positions and to obtain the electronic structure (in terms of density of states). The next step is to introduce the polymeric coating and perform classical molecular dynamics simulations with GROMACS code.

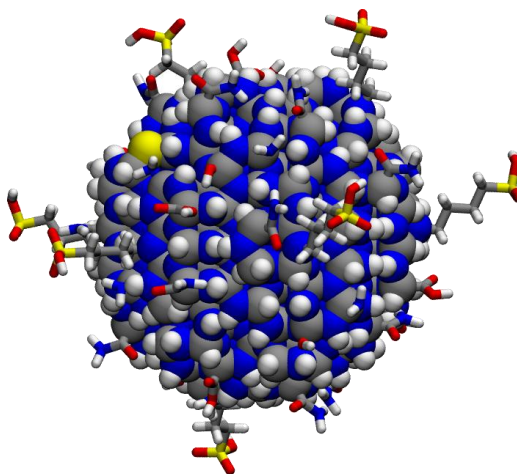


Figure 1 Ball-and-stick model of the fully optimized spherical β -C₃N₄ nanoparticle functionalized with various surface groups, obtained using CRYSTAL17 at the PBE+D3 level. Carbon, hydrogen, and nitrogen atoms are shown in grey, white, and blue respectively. Functional groups are represented as sticks, with sulfur in yellow and oxygen in red.

[1] N. Mauro, M. A. Utzeri, A. Sciortino, F. Messina, M. Cannas, R. Popescu, D. Gerthsen, G. Buscarino, G. Cavallaro and G. Giammona, *ACS Appl. Mater. & Interfaces*, **14**, 2551-2563 (2022) Decagram-Scale Synthesis of Multicolor Carbon Nanodots: Self-Tracking Nanoheaters with Inherent and Selective Anticancer Properties

Framework for Predictive Modelling of Grain Boundaries

Samira Anker^a and Christopher Race^a

^a*University of Sheffield, School of Chemical, Materials and Biological Engineering, Sir Robert Hadfield Building, Mappin Street, Sheffield, S1 3JD, United Kingdom of Great Britain and Northern Ireland*

e-mail: s.anker@sheffield.ac.uk

Metal grain boundaries are atomistic-scale defects at the interface between micron-scale grains in the material. The grains have the same lattice structure, but are rotated differently to the neighbouring grains, which can lead to dislocated atoms near the boundary, as illustrated in the figure below. Grain boundaries influence material properties including the strength, toughness, and corrosion resistance, and material behaviours such as the recovery, recrystallisation and grain growth during heat treatment.

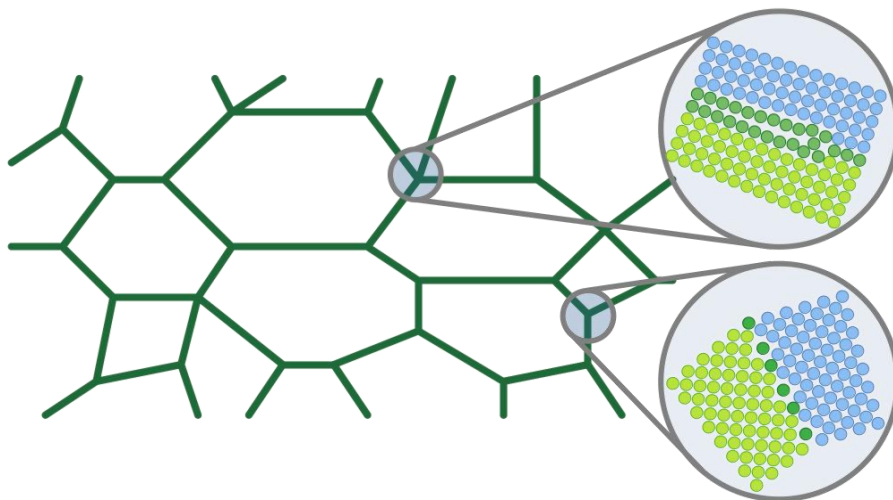


Figure: Grain boundaries in a pure metal (fcc) with atomistic level details, with the following colours: grain 1 (light blue), grain 2 (light green) and the boundary atoms (dark green).

There are many possible grain boundary structures for a pure metal and even more when impurities and alloying additions are present. The properties of grain boundaries can be modelled using density functional theory (DFT) or molecular dynamics (MD), however, many simulations are required to study the full range of possible structures, and only a small subset of structures can be captured at DFT length scales.

In this work we perform both DFT and MD simulations to investigate 160 arrangements of aluminium grain boundaries containing a single segregating copper atom. We calculate segregation energy and structural properties such as bond parameters, SOAP descriptors and Voronoi volume to compare all of the geometries. We look to apply machine learning tools to develop and test predictive models for the grain boundaries in this system. We will also present our criteria for a framework to create robust, predictive models for a given grain boundary system, whilst minimising the number of input simulations required.

First-principles Study of Perovskite Oxide for Solid Oxide Electrochemical Cells: Effects of Cation Substitution on Oxygen Ion Diffusion in $\text{Sr}_2\text{Fe}_{2-x}\text{Mo}_x\text{O}_{6-\delta}$

Sara Balocco,^{a,b,c} Francesca Fasulo,^{b,d} Ana Belén Muñoz-García,^{b,d} Michele Pavone^{b,c}

^a*Scuola Superiore Meridionale, Via Mezzocannone 4, Naples – ITALY*

^b*Consorzio Interuniversitario Nazionale per la Scienza e Tecnologia dei Materiali (INSTM), Via Giuseppe Giusti 9, Florence – ITALY*

^c*University of Naples Federico II, Department of Chemical Sciences, Via Cintia 26, Naples – ITALY*

^d*University of Naples Federico II, Department of Physics “E. Pancini”, Via Cintia 26, Naples – ITALY*

e-mail: sara.balocco@unina.it

Solid oxide fuel cells (SOFCs) and their reversible counterparts, solid oxide electrolyzer cells (SOECs), offer efficient routes for clean energy conversion water splitting and hydrogen storage.¹ However, efficient transport of oxygen ions and electrons in state-of-the-art solid-state electrolytes and electrodes typically requires high temperatures, which limit device durability and slow start-up times.

Lowering the operating temperature necessitates advanced electrode materials, particularly mixed ionic-electronic conductors (MIECs).² Among these, perovskite oxides have emerged as promising electrodes for both the oxygen evolution and reduction reactions (OER/ORR), though the efficiency of the two opposite reactions being usually largely different. $\text{Sr}_2\text{Fe}_{1.5}\text{Mo}_{0.5}\text{O}_{6-\delta}$ (SFMO) has attracted attention as a potentially bifunctional system due to its high electronic conductivity, redox-active B-site cations (Fe/Mo), and capacity to accommodate oxygen vacancies. Following previous works,^{3,4} in this study, we investigate the impact of cationic substitution on oxygen vacancy formation and migration in SFMO via first-principles calculations, targeting improved oxygen ion transport.

Two Fe:Mo ratios (1:1 and Fe-rich 3:1) are considered to assess the effect of B-site composition, while partial substitution of A-site cation (Sr) with smaller (Ca) and larger (Ba) cations at two Sr:Ca:Ba ratio (6:1:1 and 4:2:2) allowed us to probe the role of lattice strain. Structural, electronic and energetic properties are investigated using Density Functional Theory (DFT+U), revealing trends relevant to the optimization of SFMO as a bifunctional electrode material for low-temperature solid oxide technologies.

[1] A. Vojvodic, J. K. Nørskov, *Science*, **334**,1355-1356 (2011) Optimizing Perovskites for the Water-Splitting Reaction

[2] A. B. Muñoz-García, A. M. Ritzmann, M. Pavone, J. A. Keith, E. A. Carter, *Acc. Chem. Res.*, **47**, 3340-3348 (2014) Oxygen transport in perovskite-type solid oxide fuel cell materials: insights from quantum mechanics

[3] A. B. Muñoz-García, M. Pavone, E. A. Carter, *Chem. Mater.*, **23**, 4525–4536 (2011) Effect of Antisite Defects on the Formation of Oxygen Vacancies in $\text{Sr}_2\text{FeMoO}_6$: Implications for Ion and Electron Transport

[4] A. B. Muñoz-García, M. Pavone, *Chem. Mater.*, **28**, 490–500 (2016) First-Principles Design of New Electrodes for Proton-Conducting Solid-Oxide Electrochemical Cells: A-Site Doped $\text{Sr}_2\text{Fe}_{1.5}\text{Mo}_{0.5}\text{O}_{6-\delta}$ Perovskite

Computational Analysis of Energetic and Vibrational Frequencies Properties with Solvatochromic Shifts in Uracil-5Water Complexes Using DFT Methods

Asma Hennouni^a, Mohammed El Amine Benmalti^a, Claude Pouchan^b, and Panagiotis Karamanis^b

a : Laboratoire de Structure Élaboration et Applications aux Matériaux Moléculaires (SEA2M), Chemin des crêtes (Ex INES), Université Abdelhamid Ibn Badis- Mostaganem, 27000, Algeria.

b : Laboratoire de Chimie Théorique et Physico-Chimie Moléculaire – UMR 5624, Fédération de recherche IPREM 2606, Université de Pau et Pays de l'Adour, IFR – Rue Jules Ferry, 64000 Pau, France.

e-mail : amine.benmalti@univ-mosta.dz

Understanding the solvation of uracil is essential for improving hydrogen bonding (H-bonding) models in aqueous environments, with broad implications for enzymatic mechanisms and drug design. In this study, we explore novel uracil-(H₂O)_s (U5W) complexes and uncover atypical H-bonding arrangements that significantly impact vibrational properties. Density Functional Theory (DFT) calculations, employing the ωB97XD and CAM-B3LYP-D3 functionals with various basis sets, were used to identify the most stable isomers (U11333, U11133, and U12223), which feature compact water clustering and optimized H-bond lengths. Newly proposed isomers (U11134, U11144, and U11124) show greater stability than previously reported structures. Vibrational analyses confirm the influence of hydration, particularly on the ν(N–H) and ν(C2=O) stretching modes. Notably, the U12223 isomer exhibits a unique N3H⋯Ow interaction that distinctly alters its vibrational signature. These results deepen our understanding of H-bonding networks and molecular stability in solvated biomolecular systems, offering a foundation for future theoretical and experimental investigations.

Keywords: hydrogen bonding, uracil hydration, uracil–water complexes, DFT calculations, dispersion correction, infrared spectroscopy

Quantum chemistry study of water-ab initio calculation

F.Benvettou^{a,b}, S.Hiadsib, A.Bendraoua^b

^a Applied Hydrology Laboratory-department science technology -University Ain Temouchent, Bellabes Sidi Road, PO Box 284 Ain Temouchent (46000) Algeria.

^b University of Mohamed Boudiaf, USTO -BP 1505 El Mnaouer -ORAN – Algeria

e-mail: leau_lautoprotolyse@yahoo.fr

Knowledge of structures and energies of the water can provide information on the importance of interactions of several bodies. In a theoretical study, various complexes of water (OH^- , H_3O^+) with symmetry C_1 , (OH^- , H_3O^+) (H_2O) with symmetry C_1 , (OH^- , H_3O^+) (H_2O)³ with C_s symmetry; are done by Gaussian software[1], using the Berny algorithm [2] with an approach by ab initio calculations[3], using three methods: Hartree-Fock, MP2 and DFT / B3LYP with the 6-31 + G **. The analysis of results has allowed us: to determine the configurations of the coordinates representing the neutral complex (OH^- , H_3O^+) (H_2O)_n. In the comparative study of the distance of a hydrogen bond donor monomer to monomer acceptor in the neutral complex, we find that the distance O ... H successively increases with the number of water molecules added to the neutral complex (OH^- , H_3O^+) (H_2O)_n and the energy of its low hydrogen bonding more. The vibrational study of these complexes is in two parts, the first indicates the intra molecular vibrations and intermolecular second vibration. the emergence of three frequency bands (137-630, 1743-1758, 4096-4257) cm^{-1} of varying intensities, the first two bands corresponding to intra molecular vibrations, the third band corresponds to the intermolecular vibrations, the frequency bands (4096-4257) cm^{-1} meet the OH stretch vibration, the bands (1743-1758) cm^{-1} is consistent with the deformation vibration (bending), and the bands (137-630) cm^{-1} corresponds to the intra molecular vibrations of the link bridge OH .. O hydrogen. Experimental values reflect the values of frequencies calculated.

Keywords

Water, Liaison hydrogène, Ab initio, Frequency band.

Référence :

- 1 : Gaussian98. Revision.M.J.Frisch,G.W.Trucks,I.I.B.Schlegel,G.E.Scusecra,M.A.Robb, J.R.Cheeseman,V.G.Zakrzewski,J.A. Montgomery, Jr.r.e.Stratmann, J.C.Burant, S.Dapprich, J.Millam,A.D.Daniels, K.N.Kudin, M.C.Strain, O.Farkas, J.Tomasi,V.Barone,M.Cossi,R.Cammi,B.Mennucci, C.Pomelli, C.Adamo, S.Clifford, J.Ochterski, G.A.Pertersson,P.Y.Ayala,Q.Cui,K.Morokuma,D.K.Malick,A.D.Raduck,K.Raghavachari,J.B.Forestman,J.Croslovs ki,J.V.Ortiz,B.B.B.Stetanov,G.Liu,A.Liashenko,P.Piskorz,I.Komaromi,R.Gomperts,R.L.Martin,D.J.Fox,T.Keith,M. A.AiLaham,C.Y.Peng,A.Nanayakarra,C.Gonzalez,M.Challacombe,P.M.W.Gill,B.Johnson,W.Chen,M .W.Wong,J.L .Andres,L.Gonzalez,M.Head-Gordon,F.S.Replogle and J.Apople,Gaussian,Inc ; Pittsburgh PA ;(1198).
- 2 :H.B.Schlegel,J.Comput,Chem,**3**,214(1982).
- 3 : David Tozer, Chengteh Lee, George Fitzgerald, J.Chem.Phys,**104**, 14,(1996).

Applying Nudged Elastic Band in CRYSTAL: Collinear Proton Transfer Reaction Path Analysis

Francesca Capellino,^a Andreha Gelli^a, Chiara Ribaldone^a and Silvia Maria Casassa^a

University of Turin, Department of Chemistry, Via P. Giuria 5, Turin – ITALY

e-mail: francesca.capellino@edu.unito.it

In this work, the Nudged Elastic Band (NEB) method has been applied within the CRYSTAL software to characterize the transition state for the collinear proton transfer reaction $\text{H}_2 + \text{H} \rightarrow \text{H} + \text{H}_2$ and to compute its activation energy through the analysis of the reaction path. The studied reaction involves the transfer of a hydrogen atom from a H_2 molecule to a free H atom. This was the first application of the method within the NEB package recently implemented in the CRYSTAL code, necessary for the calibration of the parameters and the validation of the algorithm.

The reaction path for a particular system lies on the so-called minimum energy path (MEP) connecting two stable states.¹ In the NEB method, a set of intermediate configurations (images) of a molecular system are generated between the initial and final states. These images are connected by virtual springs and moved iteratively using projected force components derived from the energy gradient. This ensures continuity along the path, which is then optimized to find the path of least resistance, i.e., the MEP.² The procedure can be visualized using the concept of Potential Energy Surface (PES), which features local minima connected by saddle points corresponding to transition states.³

This study explores a simple collinear proton transfer reaction, while testing several key aspects of the NEB method. In particular: (i) the setting of the initial and final nuclear configurations of the reaction (ii) the number of images used in the NEB calculation to discretize the path between the two local minimum endpoints (iii) the choice of the optimization procedure (using different path optimizers) (iv) the calibration of the force constants acting between the configurations, and (v) the validation of the more sophisticated climbing image method, which improves the accuracy of transition state identification by focusing on the highest energy image along the path.⁴ All these conditions were systematically tested and compared with results obtained from the ORCA software package. The outcomes are highly encouraging: the agreement with ORCA is excellent, and the NEB implementation in CRYSTAL has proven to be stable and robust, with further consistency with previous theoretical studies.⁵

[1] S. Hayakawa, H. Xu, *Comput. Mater. Sci.*, **200**, 110785 (2021)

[2] G. Henkelman, H. Jónsson, *J. Chem. Phys.*, **113**, 9978–9985 (2000)

[3] D. G. Truhlar, in *The Encyclopedia of Physical Science and Technology*, **13**, 9-17 (2001)

[4] G. Henkelman, B. P. Uberuaga, H. Jónsson, *J. Chem. Phys.*, **113**, 9901–9904 (2000)

[5] B. S. Jursic, *J. Mol. Struct. THEOCHEM*, **427**, 117–121 (1998)

Modelling the structural and opto-electronic properties of mechanoluminochromic Cu-based Hybrid Coordination Polymers

Chiara Corapi,^a Lorenzo Gatti,^a Emma Contini,^a Sara Pandolfi,^b Giovanni Martina,^b Tommaso Salzillo,^b Elisabetta Venuti,^b Damiano Genovese,^a Chiara Gualandi,^a Lucia Maini,^a Daniele Fazzi^a

^a *University of Bologna, Department of Chemistry “G. Ciamician”, Viale P. Gobetti 85, Bologna – ITALY*

^b *University of Bologna, Department of Industrial Chemistry “Toso Montanari”, Viale P. Gobetti 85, Bologna – ITALY*

e-mail: chiara.corapi@unibo.it

Piezochromic smart coatings based on crystalline mechanoluminochromic Cu-based Hybrid Coordination Polymers (HCPs) represent a promising class of materials for stress and impact sensing through optical responses.^{1,2} Among these, [(CuI)3-BrPy]_n emerges as a particularly compelling candidate due to its distinctive photochemical properties. Under UV irradiation it demonstrates remarkable mechanochromic behavior, with its emission spectrum shifting from blue to green upon mechanical stimulation.

First-principles simulations were performed to unravel the atomistic mechanisms governing the photophysical properties of [(CuI)3-BrPy]_n, comparing the theoretical data with experimental X-Ray Diffraction, photoluminescence and Raman spectra. Starting from the HCP experimental structure, we applied a finite-size cluster approach by optimising – under certain geometrical constraints – the ground state structure at the Density Functional Theory (DFT) level, adopting a range-separated exchange-correlation functional (i.e., CAM-B3LYP).

Following ground state geometry optimization, vertical excitation energies to excited states were computed using Time Dependent DFT (TDDFT). Subsequently, the geometries of the first singlet excited state (S₁) and the first two triplet states (T₁, T₂) were optimized. This procedure allowed to hypothesize qualitative potential energy surface profiles for the ground and low-lying singlet and triplet excited states along with the Cu-I and Cu-Cu internal coordinates. The Cu-Cu distance proved to be a critical structural parameter governing the excited-state energetics. Minor variations induce pronounced changes in the excited state energies.

By comparing the experimentally observed emission wavelengths with the calculated electronic state energies, a plausible mechanism underlying the mechanochromic behavior of [(CuI)3-BrPy]_n was formulated. The origin of luminescence emissions in the ground powder could be assigned to a mixed halide-to-ligand/metal-to-ligand charge transfer triplet excited state (³XMLCT), whereas a thermally activated delayed fluorescence mechanism is predominant in the pristine material at room temperature.

These findings provide a robust framework for understanding the mechanochromic behavior of Cu-based HCPs and facilitate the rational design of advanced crystalline piezochromic coatings with tailored sensitivity for force and impact sensing applications.

[1] E. Kwon, J. Kim, K.Y. Lee and T.H. Kim, *Inorganic Chemistry*, **56**(2), 943-949 (2017) Non-phase-transition luminescence mechanochromism of a copper (I) coordination polymer

[2] A. Kobayashi, Y. Yoshida, M. Yoshida, M. Kato, *Chemistry-A European Journal*, **24**(55), 14750-14759 (2018) Mechanochromic switching between delayed fluorescence and phosphorescence of luminescent coordination polymers composed of dinuclear copper (I) iodide rhombic cores

BaFe₂Se₃: a quasi-unidimensional non-superconductor centrosymmetric

S. Deng^{*,a}, A. Roll^{*,b,c}, W. G. Zheng^{*,b}, G. Giri^a, T. Vasina^a, D. Bounoua^c, P. Fertey^d, M. Verseils^d, C. Bellin^e, A. Forget^f, D. Colson^f, P. Foury-Leylekian^b, M.B. Lepetit^{a,f}, and V. Balédent^{b,h}

^a*Institut Laue Langevin, 38000 Grenoble, France*

^b*Université Paris-Saclay, CNRS, Laboratoire de Physique des Solides, 91405, Orsay, France.*

^c*Université Paris-Saclay, CNRS-CEA, Laboratoire Léon Brillouin, 91191, Gif sur Yvette, France*

^d*Synchrotron SOLEIL, L'Orme des Merisiers, Saint Aubin BP 48, 91192, Gif-sur-Yvette, France*

^e*Université Pierre et Marie Curie, IMPMC, CNRS UMR7590, 4 Place Jussieu, 75005 Paris, France*

^f*Université Paris-Saclay, CEA, CNRS, SPEC, 91191, Gif-sur-Yvette, France.*

^g*Institut Néel, CNRS, 38042 Grenoble, France*

^h * *These authors contributed equally to this work.*

e-mail: dengs@ill.fr

Unconventional superconductivity remains one of the most emblematic quantum properties in solid-state physics, resisting any consensus on a phenomenological or microscopic model. One outstanding challenge in this field is to find the correct structure and space group symmetry. We investigated the multiferroic compound BaFe₂Se₃, which undergoes, at ambient temperature, a structural transition around 4 GPa and turns superconducting above 10 GPa and below 25 K. A combination of single crystal X-ray diffraction, Raman and Infrared spectroscopy and *ab-initio* calculations has been utilized to investigate the accurate atomic structure and lattice dynamic of BaFe₂Se₃ under pressure. We demonstrated that BaFe₂Se₃ features a non-centrosymmetric polar structure, associated with the *P2₁* space group, beyond the structural transition at 4 GPa up to the superconducting phase, making it one of the rarely known non-centrosymmetric one-dimensional superconductors. Our findings not only corrected the previously reported centrosymmetric *Cmcm* group for BaFe₂Se₃ under pressure, but also suggest profound implications for unusual superconducting states in one-dimensional case.

[1] This work has been submitted to Physical Review Letters (March 2025) and is currently under review.

Synthesis and Characterization of $\text{Na}_{10}\text{Tt}_2\text{Te}_9$ ($\text{Tt} = \text{Ge}, \text{Sn}$): Sodium Tellurotetrelate with Isolated TtTe_4 -Tetrahedra

L. Diener^a, F. Pielnhofer^a, A. Pfitzner^a

^a *University of Regensburg, Department of Inorganic Chemistry, Universitätsstr. 31 93053 Regensburg, Regensburg – Germany*

Lukas-Sebastian.Diener@Chemie.Uni-Regensburg.de

Solid electrolytes are highly promising materials for the next generation of safer and more efficient energy storage systems. Studies are more and more focusing on sodium ion conductors due to its high natural abundance, low costs, and the potential for high energy density batteries.¹

Recently the first sodium tellurosilicates with isolated $[\text{SiTe}_4]^{4-}$ tetrahedra and an isolated Te^{2-} anion was reported as $\text{Na}_{10}\text{Si}_2\text{Te}_9$.² We were able to synthesize the two heavier homologous materials $\text{Na}_{10}\text{Ge}_2\text{Te}_9$ and $\text{Na}_{10}\text{Sn}_2\text{Te}_9$. They were prepared via ball milling and subsequent high-temperature solid state reactions from the respective elements. The compounds were then analysed by X-ray diffraction and by electrochemical impedance spectroscopy. The electronic structure was investigated by density functional theory using the CRYSTAL23 code³ based on optimized structures with the functional PBE⁴, HSE06⁵, PBEsol⁶ and r²SCAN0.⁷ All three compounds crystallize isostructural in the space group $Pna2_1$ (# 33). $\text{Na}_{10}\text{Si}_2\text{Te}_9$ shows good ion conductivity at 50°C ($3.9 \times 10^{-7} \Omega^{-1} \text{cm}^{-1}$).² $\text{Na}_{10}\text{Ge}_2\text{Te}_9$ and $\text{Na}_{10}\text{Sn}_2\text{Te}_9$ also show moderate to good ionic conductivity.

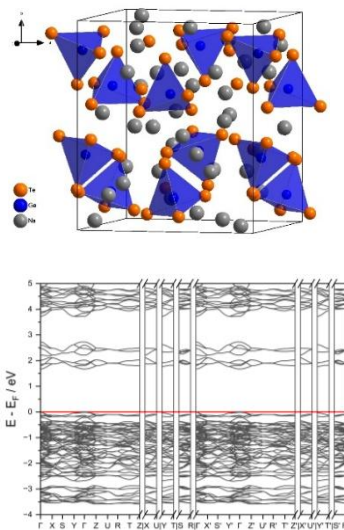


Figure 2. Band structure of $\text{Na}_{10}\text{Ge}_2\text{Te}_9$.

- [1] S. Kasap and P. Capper, *Springer International Publishing*, Cham, 2017, Springer Handbook of Electronic and Photonic Materials.
- [2] F. Kamm, F. Pielnhofer, M. Schlosser and A. Pfitzner, *Dalton Trans.*, **53**, 15630–15637, (2024), Enhanced sodium ion mobility in sodium tellurosilicates and crystal structures of Na_4SiTe_4 and $\text{Na}_{10}\text{Si}_2\text{Te}_9$ with isolated $[\text{SiTe}_4]^{4-}$ tetrahedra and isolated Te^{2-} anions.
- [3] A. Erba, J. K. Desmarais, S. Casassa, B. Civalleri, L. Donà, I. J. Bush, B. Searle, L. Maschio, L. Edith-Daga, A. Cossard, C. Ribaldone, E. Ascrizzi, N. L. Marana, J.-P. Flament and B. Kirtman, *J. Chem. Theory Comput.*, **19**, 6891–6932, (2023), CRYSTAL23: A Program for Computational Solid State Physics and Chemistry.
- [4] Perdew, J. P.; Burke, K.; Ernzerhof, M. Generalized Gradient Approximation Made Simple. *Phys. Rev. Lett.*, **77**, 3865–3868, (1996), Generalized Gradient Approximation Made Simple.
- [5] J. Heyd, J. E. Peralta, G. E. Scuseria and R. L. Martin, *J. Chem. Phys.*, **123**, 174101, (2005), Energy band gaps and lattice parameters evaluated with the Heyd-Scuseria-Ernzerhof screened hybrid functional.
- [6] Perdew, J. P.; Ruzsinszky, A.; Csonka, G. I.; Vydrov, O. A.; Scuseria, G. E.; Constantin, L. A.; Zhou, X. and Burke, K. *Phys. Rev. Lett.*, **100**, 136406, (2008), Restoring the Density-Gradient Expansion for Exchange in Solids and Surfaces.
- [7] Markus Bursch, Hagen Neugebauer, Sebastian Ehlert, and Stefan Grimme; *The Journal of Chemical Physics*, **156**(13):134105, (2022); Dispersion corrected r2scan based global hybrid functionals: r2scanh, r2scan0, and r2scan50.

Synthesis and Characterization of Halocuprates(I)

L. Dopfer,^a F. Pielhofer^a, A. Pfitzner^a

^aUniversity of Regensburg, Department of Inorganic Chemistry, Albertus-Magnus-Straße 4, Regensburg – Germany

e-mail: Lukas.Dopfer@chemie.uni-regensburg.de

Halocuprates(I), featuring copper(I) ions coordinated by halide ligands, exhibit a wide range of structural motifs. These can range from simple monomers to complex polymeric frameworks (Figure 1), which makes rational crystal engineering challenging. These compounds are of interest due to their electronic properties, luminescence behavior and potential applications in optoelectronic devices.^{1, 2}

In this study, the novel bis(1-methyl-1-isopropylpyrrolidinium) di- μ -iodo-diiododicuprate(I) (**A**) has been successfully synthesized under solvothermal reaction conditions with acetone as a solvent. The crystal structure (Figure 2) was determined by single crystal X-ray diffraction and the phase purity of the compound was confirmed via powder X-ray diffraction. The luminescence properties of the new compound were investigated by UV/VIS-spectroscopy and emission spectra both by room temperature and at 77 K.

First principles calculations of the new compound were carried out, by using the CRYSTAL23 software³, with an emphasis on geometry optimization and the evaluation of electronic properties at various levels of theory.

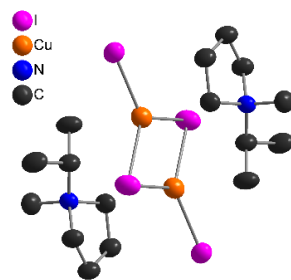


Figure 1: Smallest complete unit of **A**.

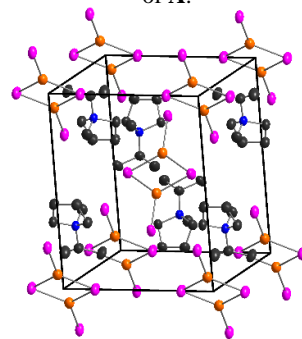


Figure 2: Unit cell of **A**.

[1] C. Hasselgren Arnby, S. Jagner, I. Dance, *Cryst. Eng. Comm.*, **6**, 257 (2004) Questions for crystal engineering of halocuprate complexes: concepts for a difficult system.

[2] M. J. Leidl, D. M. Zink, A. Schinabeck, T. Baumann, D. Volz, H. Yersin, *Top. Curr. Chem.*, **25**, 374 (2016) Copper(I) Complexes for Thermally Activated Delayed Fluorescence: From Photophysical to Device Properties.

[3] A. Erba, J. K. Desmarais, S. Casassa, B. Civalleri, L. Donà, I. J. Bush, B. Searle, L. Maschio, L.-E. Daga, A. Cossard, C. Ribaldone, E. Ascrizzi, N. L. Marana, J.-P. Flament, B. Kirtman, *J. Chem. Theory Comput.* **19**, 6891–6932 (2023) CRYSTAL23: A Program for Computational Solid State Physics and Chemistry.

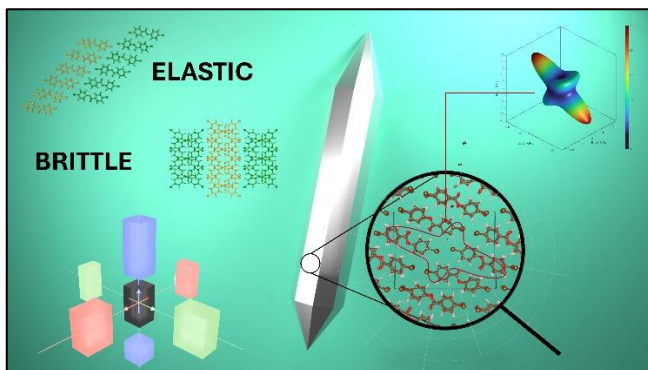
Evaluating Mechanical Behavior in Organic Molecular Crystals Through Computational Modeling

Tea Frey,^a Ivan Kodrin

^aUniversity of Zagreb, Faculty of Science, Department of Chemistry, Horvatovac 102a, Zagreb – Croatia

e-mail: tfrey@chem.pmf.hr

Organic crystalline materials are gaining attention for their potential use in advanced technologies, including stimuli-responsive materials, organic electronics, nanomachinery, pharmaceuticals, etc. However, their inherent brittleness remains a significant limitation. The understanding of mechanical flexibility in crystals plays a key role in their applicability and integration in everyday use. Mechanical properties like elasticity and plasticity can be correlated to molecular structure and intermolecular interactions.¹ The impact of crystal packing on mechanical properties can be explored through polymorphism. In this work, a series of *p*-halogenated benzene-based esters are used to computationally explore how chemical structure and polymorphism impact the elasticity of organic molecular crystals. Bromine derivatives have already been shown to exhibit multiple polymorphs, some of excellent flexibility and others of brittle nature.² By varying *para*-substituted halogens (chlorine, bromine and iodine), we investigate how subtle changes in molecular structure impact molecular packing and flexibility of synthesized materials. To predict and rationalize the mechanical response, we use periodic DFT methods implemented in CRYSTAL23 program. Crystal structures are optimized, and a series of properties is explored using PBE-D3 functional and pob-TZVP-rev2 basis set. For each structure, Young's moduli are computed and correlated with the interaction energies of chosen unit cell fragments. Furthermore, we investigate crystalline properties by applying virtual tensile tests, designed to explore crystal structure deformation along specific directions orthogonal to crystallographic planes. Our work is complemented experimentally by discovering new crystal structures and polymorphs of studied compounds with different mechanical properties. Through this combined approach, we are one step closer to establishing a computational framework capable of explaining how subtle changes in molecular structures and polymorphic rearrangements can affect the mechanical properties of organic crystals.



- [1] M. Đaković, M. Pisačić, M. Borovina, I. Kodrin and T. Frey, *J. Am. Chem. Soc.*, **147** (25), 22219–22227 (2025) Unveiling Structure-Dynamic Processes in Crystals of 1D Cd(II) Coordination Polymers during the Elastic Flexible Events
- [2] S. Saha, G. R. Desiraju, *Chem. Commun.*, **54**, 6348–6351 (2018) Trimorphs of 4-bromophenyl 4-bromobenzoate. Elastic, brittle, plastic

Ab Initio Tools for XANES & EXAFS simulations

Beatrice Garetto^a, Ning Cao^{b,c}, Valeria Finelli^a, Erlend Aunan^b, Matteo Signorile^a, Unni Olsbye^a, Silvia Bordiga^a, Ainara Nova^{b,c}, Elisa Borfecchia^a

^aDepartment of Chemistry, NIS and INSTM Reference Centre, Università di Torino, I-10125 Turin, Italy

^bSMN Centre for Material Science and Nanotechnology, Department of Chemistry, University of Oslo, N-0315 Oslo, Norway

^cHylleraas Centre for Quantum Molecular Sciences, Department of Chemistry, University of Oslo, N-0315 Oslo, Norway

e-mail: beatrice.garetto@unito.it

In recent years, X-ray absorption spectroscopy (XAS) has become a key technique for investigating the structure and composition of materials, providing insights into active sites under in situ/operando conditions¹. XAS spectra are typically divided into two regions: XANES, sensitive to oxidation state and electronic structure, and EXAFS, which provides information on interatomic distances and local disorder¹. Experimentally, XANES is easier to acquire with high quality, while EXAFS requires broader energy ranges and higher signal-to-noise ratios. A major challenge in XAS lies in its intrinsically averaged signal, reflecting contributions from all absorber-containing species in the sample. To disentangle overlapping

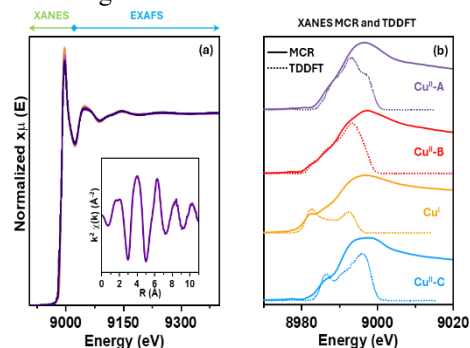


Figure 1: (a) XAS spectra and (b) MCR-TDDFT case study by Garetto et al.,¹ where the limitation of the simulation is visible above the edge.

features, multivariate methods—particularly Multivariate Curve Resolution (MCR)¹—are widely used. In addition, the applicability of MCR in the EXAFS region is often limited by experimental constraints. To overcome these analytical and interpretative limitations, *ab initio* simulations provide a powerful framework by delivering theoretical reference spectra and structural models that can be directly compared to experimental data. In this context, MCR-derived XAS spectra can also serve as a reliable benchmark for selecting representative structures to be used in *ab initio* calculations. When data quality permits, EXAFS can provide the structural data (1st-2nd-3rd shell interatomic distances) needed for the design of target structures. This study reports the complementarity between two widely used *ab initio* tools for

XAS simulation: ORCA, based on time-dependent density functional theory (TD-DFT)², and FDMNES³. TD-DFT is particularly well suited for simulating the XANES region, as it allows for an accurate description of discrete core-to-bound-state transitions and localized excited states. However, it becomes less reliable in the vicinity of and beyond the absorption edge, where the photoelectron is promoted to the continuum and exhibits quasi-free behaviour—conditions that would require significant approximations within a TD-DFT framework. To address this limitation, FDMNES offers a robust alternative for modelling the edge and EXAFS regions. It employs the finite difference method (FDM) to numerically solve the Schrödinger equation for the photoelectron, without resorting to the muffin-tin approximation, which assumes spherically symmetric atomic potentials and may compromise accuracy. The development of FDMX³ (introduced in 2015) has further extended these capabilities. By combining the strengths of ORCA and FDMNES, it becomes possible to integrate both electronic and structural accuracy, resulting in comprehensive and reliable simulations of XAS spectra across their full energy range.

[1] B. Garetto, et al., *J. Phys. Chem. C*, **129**(7), 3570-3582 (2025) Pinpointing Cu-Coordination Motifs in Bio-Inspired MOFs by Combining DFT-Assisted XAS Analysis and Multivariate Curve Resolution.

[2] F. Neese, *J. Chem. Phys.*, **152**, 224108 (2020) The ORCA quantum chemistry program package.

[3] S. A. Guda, et al., *J. Chem. Theory Comput.*, **11**, 4512-4521 (2015) Optimized Finite Difference Method for the Full-Potential XANES Simulations: Application to Molecular Adsorption Geometries in MOFs and Metal-Ligand Intersystem Crossing Transients.

Structural Characterization, Electronic Properties and Space Group Stability of LiBaAs Based on DFT Calculations

Elisabeth Huf,^a Arno Pfitzner^a

^aUniversity of Regensburg, Department of Inorganic Chemistry, Universitätsstraße 31, Regensburg – GERMANY

e-mail: elisabeth.huf@ur.de

The compound LiBaAs was investigated with respect to its crystal structure, electronic properties and impedance behavior. The compound was synthesized via ball milling of stoichiometric amounts of the elements and high-temperature treatment. LiBaAs crystallizes in the space group $P6_3/mmc$ (No. 194), characterized by layers of lithium and arsenic separated by barium atoms. Each barium atom resides within a hexagonal prism formed by six lithium and six arsenic atoms, while arsenic is coordinated by six barium atoms and three lithium atoms in a trigonal prismatic geometry. Experimentally determined lattice parameters are $a = 4.6366(1) \text{ \AA}$ and $c = 8.7294(2) \text{ \AA}$, $V = 162.52(5) \text{ \AA}^3$. In comparison, literature reports indicate that LiBaAs crystallizes in the space group $P\bar{6}m2$ (No. 187) with the lattice parameters $a = 4.622(2) \text{ \AA}$, $c = 4.364(2) \text{ \AA}$ and $V = 80.8 \text{ \AA}^3$.¹ Impedance spectroscopy confirms the semiconducting nature of LiBaAs, with specific conductivity ranging from $3.2 \times 10^{-8} \Omega^{-1} \text{cm}^{-1}$ at 40°C to $4.3 \times 10^{-4} \Omega^{-1} \text{cm}^{-1}$ at 300°C . Density functional-based quantum chemical calculations using CRYSTAL23² were performed to calculate the band gap of the compound and to compare the energetic difference of the experimentally observed space group $P6_3/mmc$ (No. 194) with the literature reported space group $P\bar{6}m2$ (No. 187).¹

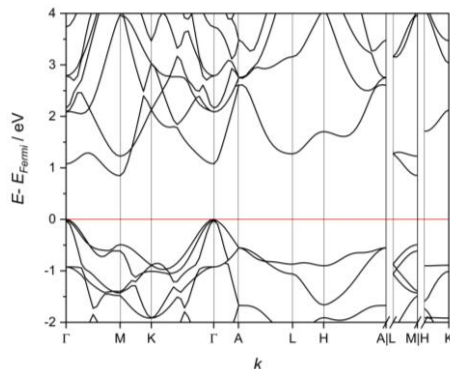


Figure 1: Band structure of LiBaAs.

[1] J.H. Albering, T. Ebel and W. Jeitschko, *Z. Kristallogr.*, **S12**, 242b (1997) Präparation, Kristallstruktur und magnetische Eigenschaften der Verbindungen LiAX (A= Ca, Sr, Ba, Eu, Yb; X= P, As, Sb, Bi).

[2] A. Erba, J. K. Desmarais, S. Casassa, B. Civalleri, L. Donà, I. J. Bush, B. Searle, L. Maschio, L. Edith-Daga, A. Cossard, C. Ribaldone, E. Ascricchi, N. L. Marana, J.-P. Flament and B. Kirtman, *J. Chem. Theory Comput.*, **19**, 6891–6932 (2023) CRYSTAL23: A Program for Computational Solid State Physics and Chemistry.

Thermoelectric Performance of Sb Doped ZnO Thin Films Insights from Density Functional Theory and Boltzmann Transport Calculations

Misha Khalid^a, Ankur Chatterjee^{a,b}, Hadiqa Naaz^c, Yasmine Salaki^d, Carlos J. Tavares^e, Michał Pawlak^{a*}

^a*Institute of Physics, Faculty of Physics, Astronomy and Informatics, Nicolaus Copernicus University in Toruń, Grudziądzka 5, 87-100 Toruń, Poland*

^b*Chair of Applied Solid-State Physics, Experimental Physics VI, Ruhr-University Bochum, Universitätsstrasse 150, D-44780 Bochum, Germany.*

^c*School of Interdisciplinary Engineering & Science (SINES), National University of Sciences and Technology (NUST), H-12, Islamabad, 44000, Pakistan.*

^d*Department of Physics, Quaid-i-Azam University Islamabad, National Center for Physics Islamabad 44000, Pakistan.*

^e*Centre of Physics of Minho and Porto Universities (CF-UM-UP), University of Minho, 4804-533 Guimarães, Portugal*

e-mail: mishakhalid@doktorant.umk.pl

This study investigates the thermoelectric properties of antimony-doped zinc oxide (ZnO:Sb) thin films using density functional theory calculations with Quantum ESPRESSO and BoltzTraP codes. Electronic band structure, phonon dispersion, and thermoelectric transport coefficients were computed for pristine ZnO and 2% Sb-doped ZnO ($3 \times 3 \times 1$ supercell). Results show that Sb doping creates shallow acceptor states near the Fermi level, increasing hole concentration and enabling p-type conduction. Both systems exhibit metallic behavior with no band gap. Sb incorporation disrupts lattice periodicity, significantly reducing thermal conductivity while maintaining enhanced electrical conductivity. The thermoelectric figure of merit (ZT) at 300 K shows substantial improvement over undoped ZnO. The findings demonstrate ZnO:Sb thin films as promising thermoelectric materials with optimized electronic and thermal transport properties suitable for energy conversion applications.

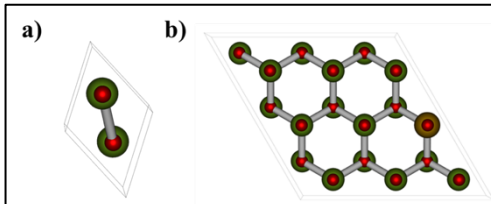


Figure 1. ZnO atomic structure: **a)** unit cell, **b)** 2% Sb-doped supercell ($3 \times 3 \times 1$). Green = Zn, red = O, golden = Sb.

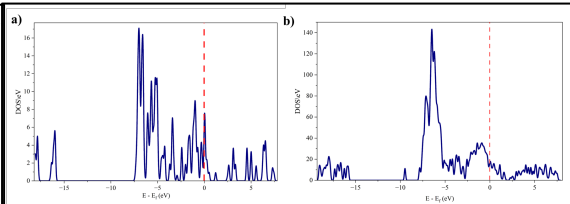


Figure 2: (TDOS) for **(a)** pristine ZnO and **(b)** 2% Sb-doped ZnO ($3 \times 3 \times 1$ supercell). Fermi level at 0 eV (red dashed line). Sb doping modifies electronic states near the Fermi level.

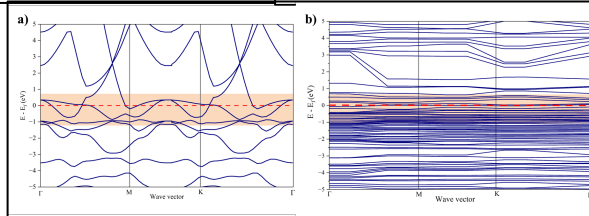


Figure 3: Electronic band structure of ZnO. **(a)** Pristine ZnO; **(b)** 2% Sb-doped ZnO in a $3 \times 3 \times 1$ supercell

Elastic properties of Iron-Sulfur alloys at Extreme Conditions

Dennis Kosobokov^a, Xiang Li^a, Lianjie Man^b, Georgios Aprilis^a, Susanne C. Müller^a, Katarzyna Skrzynska^a, Ilya Kupenko^a

^aESRF The European Synchrotron, 71 Avenue des Martyrs, Grenoble France

^bBayerisches Geoinstitut, Universität Bayreuth, Germany

e-mail: dennis.kosobokov@esrf.fr

Iron-nickel alloys are the primary components of the cores of terrestrial planets, such as Earth. However, seismic models¹ reveal a density deficit and reduced seismic velocities in Earth's core compared to pure Fe-Ni alloys, suggesting the presence of 4–7 wt% of light elements such as S, C, O, H, and Si. The concentration and combination of these light element candidates remain unknown^{2,3}.

Despite extensive discussion of sulfur as a plausible alloying element, experimental data remain scarce, and our knowledge of the Fe-S systems mainly arises from theoretical models that are highly constrained and include numerous assumptions.^{4,5} Most available experimental studies focus on the high-pressure/high-temperature behaviour of classical iron sulfide and iron-rich sulfide phases (FeS, Fe₂S, Fe₃S).^{6,7} Investigations of iron-sulfur alloys on the iron-rich side of the phase diagram are hindered by the insolubility of sulfur in iron at ambient pressure. However, the maximum solubility of sulfur in solid iron increases with pressure, rising from 0.8 wt% sulfur at 25 GPa⁸ to about 4 wt% at 250 GPa.⁹

To better constrain the sulfur content in terrestrial planetary cores, we investigated the elastic properties of an iron alloy containing 1 wt% sulfur, pre-synthesized in a multi-anvil press, at high pressures using synchrotron X-ray diffraction in diamond anvil cells. We then extrapolated the measured elastic parameters to planetary core conditions. In this contribution, we will present the elastic behavior of iron-sulfur alloys under extreme conditions and compare our findings to available seismic models. Our results provide new constraints on the sulfur budget in the interior of terrestrial planets.

- [1] A. M. Dziewonski, D. L. Anderson, *Physics of the Earth and Planetary Interiors*, **25**, 297, (1981) Preliminary reference Earth model.
- [2] K. Hirose, B. Wood, L. Vočadlo, *Nat Rev Earth Environ*, **2**, 645, (2021) Light elements in the Earth's core.
- [3] J.-P. Poirier, *Physics of the Earth and Planetary Interiors*, **85**, 319, (1994) Light elements in the Earth's core: A critical review.
- [4] Z. G. Bazhanova, V. V. Roizen, A. R. Oganov, *Phys.-Usp.*, **60**, 1025, (2017) High-pressure behavior of the Fe-S system and composition of the Earth's inner core.
- [5] S. Ono, A. R. Oganov, J. P. Brodholt, L. Vočadlo, I. G. Wood, A. Lyakhov, C. W. Glass, A. S. Côté, G. D. Price, *Earth and Planetary Science Letters*, **272**, 481, (2008) High-pressure phase transformations of FeS: Novel phases at conditions of planetary cores.
- [6] C. C. Zurkowski, B. Lavina, S. Chariton, S. Tkachev, V. B. Prakapenka, A. J. Campbell, *American Mineralogist*, **107**, 739 (2022) The crystal structure of Fe₂S at 90 GPa based on single-crystal X-ray diffraction techniques.
- [7] S. J. Kuhn, M. K. Kidder, D. S. Parker, C. dela Cruz, M. A. McGuire, W. M. Chance, L. Li, L. Debeer-Schmitt, J. Ermentrout, K. C. Littrell et al., *Physica C: Superconductivity and its Applications*, **534**, 29, (2017) Structure and property correlations in FeS.
- [8] J. Li, Y. Fei, H. K. Mao, K. Hirose, S. R. Shieh, *Earth and Planetary Science Letters*, **193**, 509, (2001) Sulfur in the Earth's inner core.
- [9] Y. Mori, H. Ozawa, K. Hirose, R. Sinmyo, S. Tateno, G. Morard, Y. Ohishi, *Earth and Planetary Science Letters*, **464**, 135, (2017) Melting experiments on Fe-Fe₃S system to 254 GPa.

Shedding Light on Photocatalysis by Cobalt Complexes: a Computational Study

Sofia Lerda,^a Ahmet Altun^b and Giovanni Bistoni^{*a}

^a University of Perugia, Department of Chemistry, Biology and Biotechnology, Via dell'Elce di Sotto 8, 06123, Perugia – Italy

^b Max-Planck-Institut für Kohlenforschung, Kaiser-Wilhelm-Platz 1, D-45470, Mülheim an der Ruhr – Germany

e-mail: sofia.lerda@dottorandi.unipg.it

In a recent study, a cobalt-catalyzed, light-induced synthesis of amides, achieving 100% atom economy by coupling amines and alkenes under 390 nm LED illumination, was reported¹.

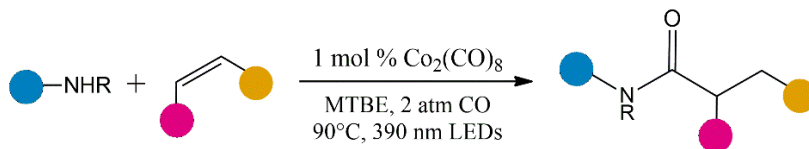


Figure 1. Cobalt-catalyzed synthesis of amides by hydroaminocarbonylation under mild conditions promoted by light.

Despite its practical appeal, important mechanistic questions remain, particularly regarding the photo-induced generation of the active catalyst and the subsequent catalytic cycle. Herein, we shed light onto the mechanism of this transformation. Our results revealed how vibronic and spin-orbit coupling effects synergistically enhance the photoabsorption of the precatalyst at 390 nm, driving the formation of the active species, $[\text{Co}(\text{CO})_3]^-$. These insights may extend to a broader range of cobalt-catalyzed transformations² where photochemical activation follows a similar pathway. Furthermore, we identify an amine-assisted nucleophilic substitution as the most favorable pathway for amide formation over a reductive elimination pathway which involves prohibitively high activation barriers. We thus propose nucleophilic substitution as a general mechanistic motif for product formation and catalyst regeneration in other hydrocarbonylations catalyzed by $[\text{Co}(\text{CO})_3]^-$.

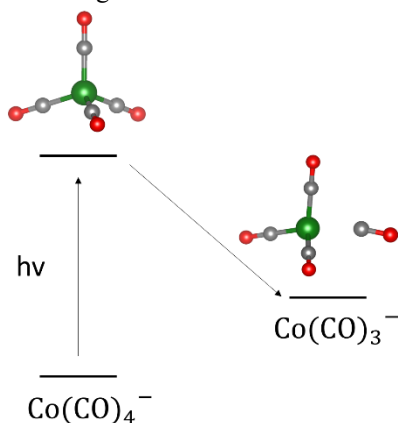


Figure 2. Proposed role of light absorption in the formation of the active species.

[1] M.S. Faculak, A.M. Veatch and E.J. Alexanian, *Science*, **383**, 77-81 (2024) Cobalt-Catalyzed Synthesis of Amides from Alkenes and Amines Promoted by Light.

[2] M.S. Faculak, M.R. Rodriguez and E.J. Alexanian, *J. Am. Chem. Soc.*, **147**, 14060-14064 (2025) Cobalt-Catalyzed Syntheses of Esters and Carboxylic Acids from Alkenes Promoted by Light.

Second hyperpolarizability of organic solvent molecules in vacuum, in liquid and in crystal

Igors Mihailovs,^a Dmitry Bocharov^a and Sergei Piskunov^a

^a*University of Latvia, Institute of Solid State Physics, Kengaraga St 8, Riga – LATVIA*

e-mail: igors.mihailovs@cft.lu.lv

There is a constant interest in third-order nonlinear optics in the research community. We compared the second hyperpolarizability calculated in vacuum, in liquid and in crystal for multiple solvent molecules. Effect of vacancy defects present in crystals were also explored.

Exploring the Electronic Properties of HKUST-1: An Experimental and Computational Study

F. Mondaca^a, L. A. Alfonso Herrera^b, M. Arias^c and S. Conejeros^c

^aUniversidad San Sebastián, Facultad de Ingeniería, Lago Panguipulli 1390, Puerto Montt – Chile

^bUniversidad Autónoma de Nuevo León, Facultad de Ingeniería Civil, Av. Universidad S/N Ciudad Universitaria, San Nicolás de los Garza, Nuevo León – México

^cUniversidad Católica del Norte, Departamento de Química, Av. Angamos 0610, Antofagasta – Chile

e-mail: felipe.mondaca@uss.cl

In this work, we present a combined experimental and computational study on the HKUST-1 metal-organic framework (MOF), aimed at understanding the physicochemical factors that limit its photocatalytic performance. Experimentally, we synthesized HKUST-1 via a slow evaporation method and confirmed its structure and morphology through X-ray diffraction (XRD) and scanning electron microscopy (SEM). Optical properties were investigated using UV-Vis spectroscopy and Kubelka-Munk analysis, and photocatalytic activity was evaluated through hydrogen evolution measurements under light irradiation. From a theoretical perspective, density functional theory (DFT) calculations were employed to analyze the electronic structure, including the density of states (DOS), band structure, and magnetic ordering (FM vs. AFM). The results indicate that key limitations in photocatalytic performance are associated with the wide bandgap, low relative permittivity, and conduction band position. These findings are supported by both experimental and theoretical evidence, offering insights into the structural and electronic factors governing the activity of HKUST-1, and highlighting its potential for photoelectrochemical oxidation processes.

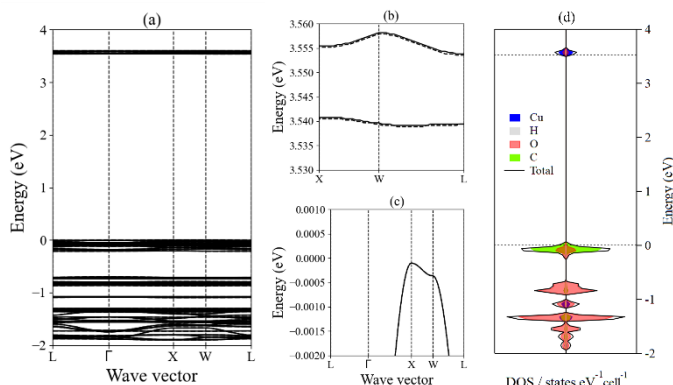


Figure 1. (a) Energy band structure (b) magnification of the conduction band, (c) magnification of the valence band, and (d) density of state of HKUST-1 calculated with HSE06 functional¹.

[1] L. A. Alfonso Herrera et. al., *New J. Chem.*, **48**, 11377-11386 (2024) Elucidating, understanding, and correlating the (photo)electrochemical and physicochemical properties of HKUST-1 through an experimental and computational approach

Understanding Structure–Property Relationships in Coordination Polymers with CRYSTAL23

Filippo Monti, Vasiliki Benekou, Andrea Candini and Vincenzo Palermo

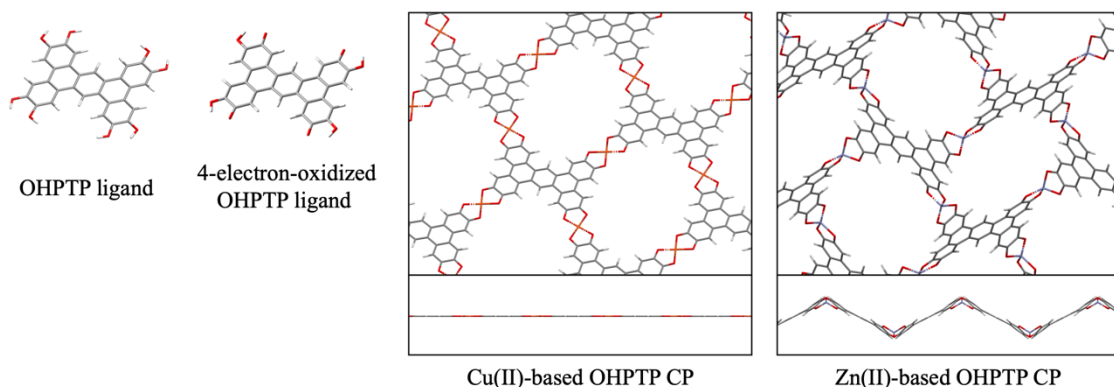
National Research Council of Italy, Institute for Organic Synthesis and Photoreactivity,
Via Piero Gobetti 101, 40129 Bologna – ITALY

e-mail: filippo.monti@cnr.it

Coordination polymers (CPs) offer a versatile platform for designing functional materials with tunable electrical and structural properties. However, establishing a predictive link between coordination geometry and macroscopic behavior remains a major challenge. In this work, we investigated how subtle differences in metal-ligand interactions — specifically between Cu(II) and Zn(II) ions coordinating a π -conjugated organic ligand (OHPTP) — affect the structural order, electronic transport, and thermal stability of CP thin films. [1]

We synthesized Cu- and Zn-based CPs via shear-coating technique, ensuring uniform film formation. XPS, FT-IR, UV-vis, and conductive AFM measurements revealed that Cu(II) readily forms planar, highly ordered CPs with high electrical conductivity, while Zn(II) is hardly included into the CP inducing disordered structures with poor π - π stacking and negligible conductance. CRYSTAL23 calculations were key to interpreting these results: we modeled the coordination polymers as 2D periodic layers, comparing ideal monolayers and partially metal-loaded structures at different ion-to-ligand ratios.

The DFT results show that the OHPTP ligand requires partial oxidation to form the related Cu(II) and Zn(II) CPs. The former metal displays a square-planar coordination, resulting in flat, π -conjugated layers with narrow band gaps and dispersive valence/conduction bands; in contrast, Zn(II) coordination induces a non-planar, tetrahedral geometry, forcing the ligand network into a zig-zag arrangement with significantly reduced band dispersion. Even at partial ion loading, Zn(II) coordination already leads to a severe tilting, whereas Cu(II) preserves planarity.



[1] V. Benekou, Z. Zhang, L. Sporrer, A. Candini, F. Monti, A. Kovtun, F. Liscio, S. C. B. Mannsfeld, X. Feng, R. Dongd and V. Palermo, *Nanoscale*, **17**, 14816-14826 (2025).

Synthesis and Characterisation of Na_5TrSe_4 ($\text{Tr} = \text{Al}, \text{In}$): Sodium Selenidotrirelates with Isolated TrSe_4 Tetrahedra

G. Nowotny,^a F. Pielenhofer,^a A. Pfitzner^a

^aUniversity of Regensburg, Department of Inorganic Chemistry, Albertus Magnus Straße 4, Regensburg – Germany

e-mail: georg.nowotny@chemie.uni-regensburg.de

All-solid-state batteries (ASSB) use solid electrolytes in favour of liquid electrolytes promising enhanced safety and higher energy density. Sodium-based solid electrolytes are considered a cost-effective and resource-efficient alternative to conventional lithium-based electrolytes.¹

The ternary compounds Na_5AlSe_4 and Na_5InSe_4 were synthesised via ball milling and subsequent high-temperature solid state reaction from stoichiometric amounts of the respective elements. The crystal structures were analysed by X-ray diffraction and electrochemical impedance spectroscopy. Na_5AlSe_4 crystallises in the space group $Pbca$ (No. 61) and Na_5InSe_4 in $Pnma$ (No. 62). The anionic substructure comprises isolated $[\text{TrSe}_4]^{5-}$ tetrahedra embedded in a cationic matrix. The sodium ions form distorted tetrahedra and octahedra with nearby selenides. Na_5AlSe_4 shows good ionic conductivity at 50 °C ($1.3 \times 10^{-7} \text{ Scm}^{-1}$) whereas Na_5InSe_4 shows moderate ionic conductivity at 50 °C ($5.0 \times 10^{-9} \text{ Scm}^{-1}$).

The electronic properties were investigated by density functional theory using the CRYSTAL23 code², based on optimised structures at different levels of theory.

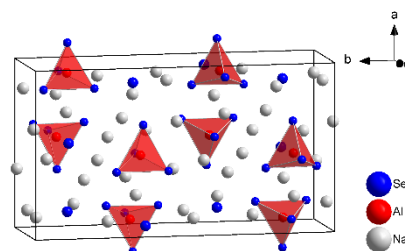


Figure 1: Crystal structure of Na_5AlSe_4

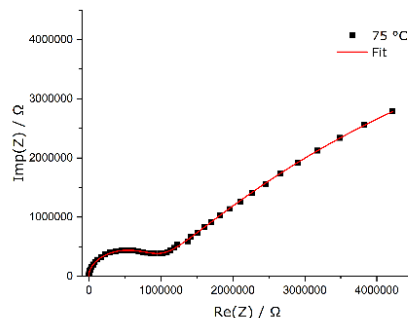


Figure 2: Nyquist plot at 75 °C of Na_5AlSe_4 with the corresponding circuit diagram.

[1]: Hwang J.; Myung S.; Sun Y.; *Chem. Soc. Rev.*, **46**, 3529-3614 (2017) Sodium-ion batteries: present and future.

[2]: A. Erba, J. K. Desmarais, S. Casassa, B. Civalleri, L. Donà, I. J. Bush, B. Searle, L. Maschio, L. Edith-Daga, A. Cossard, C. Ribaldone, E. Ascrizzi, N. L. Marana, J.-P. Flament and B. Kirtman, *J. Chem. Theory Comput.*, **19**, 6891–6932 (2023), CRYSTAL23: A Program for Computational Solid State Physics and Chemistry.

Modulating Two-Photon Absorption in a Pyrene-based MOF series: Structure-Property Relationships

Helmy Pacheco Hernández,^a Simon N. Deger,^b Yang Cui,^b Hongxing Hao,^b Vanessa Ramm,^b David C. Mayer,^b Khai-Nghi Truong,^c Alexander Pöthig,^b Jürgen Hauer,^b Mariana Kozłowska,^a and Roland A. Fischer^b

^aKarlsruhe Institute of Technology (KIT), Institute of Nanotechnology (INT), Kaiserstraße 12, 76131, Karlsruhe – Germany

^bTechnical University of Munich (TUM), School of Natural Sciences, Department of Chemistry, Catalysis Research Center, 85747, Garching – Germany

^cRigaku Europe SE, Hugentottenallee 167, 63263 Neu-Isenburg – Germany

e-mail: helmy.hernandez@kit.edu

Nonlinear optical properties in photoactive materials arise from their interaction with intense laser fields, enabling a range of phenomena.^[1] In the field of nonlinear optics (NLO), multiphoton absorption (MPA) has recently attracted considerable attention due to its role in numerous applications^[2] (e.g., deep tissue imaging and fluorescence microscopy),^[3] medicine (e.g., photodynamic therapy),^[4] materials science (e.g., 3D microfabrication),^[5] and photonics (e.g., optical limiting).^[6] Due to the wide range of interdisciplinary applications, significant research has focused on understanding and improving the MPA properties of various material classes.^[2a] These include inorganic systems like nanocrystals, quantum dots, nanowires, perovskites, and metal clusters, as well as organic materials such as chromophores, dendrimers, and polymers.^[2a, 7] More recently, attention has shifted toward hybrid materials such as Metal-Organic Frameworks (MOF).^[8]

MOFs offer several advantages for enhancing MPA, including controlled chromophore aggregation and improved stability.^[9] This is typically achieved by attaching coordinating groups (e.g., carboxylic acids) to chromophores, which then bind to secondary building units (SBUs), often metal-oxo clusters. These clusters act as nodes that connect organic linkers, stabilizing the chromophores within a rigid framework.^[10] MOFs are a good alternative to investigate structure-property relationships affecting MPA.^[8b] Framework materials that incorporate anthracene-, carbazole-, or aggregation-induced emission (AIE) dyes, particularly those based on tetra(4-carboxylphenyl)ethylene, have demonstrated exceptional two-photon absorption (2PA) activity, reaching values as high as 7.4×10^7 Göppert-Mayer (GM) units in dense Zn-MOFs^[11] ($1 \text{ GM} = 10^{-50} \text{ cm}^4 \cdot \text{s} \cdot \text{photon}^{-1} \cdot \text{molecule}^{-1}$). However, establishing clear structure-property correlations remains difficult due to the many intertwined factors that influence 2PA.^[8b, 11c]

Several key features have been identified to enhance the 2PA cross-section $\sigma^{(2)}$ of chromophores embedded in MOFs,^[8b] including increased linker rigidity (which suppresses non-radiative decay), polarization effects induced by the SBU, and especially intermolecular interactions among closely packed chromophores.^[11b, 11c, 11e] Still, the precise role of these interactions and their interplay remains poorly understood due to the complexity of the systems involved.^[8b, 11i]

In this study, we investigate how different structural arrangements influence 2PA activity by analyzing the polymorphs NU-1000 and NU-901. These MOFs share the same stoichiometry, incorporating the linker 1,3,6,8-tetrakis(p-benzoic acid)pyrene (H₄TBAPy) and a zirconium-oxo SBU, but differ in the orientation of their linkers. This allows for a direct comparison of their structure-property relationships. Additionally, we explore SrTBAPy and BaTBAPy, two MOFs with the same linker but different SBUs based on Sr and Ba, which result in denser topologies and reduced inter-linker distances.

Time-dependent density functional theory (TD-DFT) calculations were performed to evaluate the electron density changes and quantify charge transfer. Our results show that in BaTBAPy, the shorter distances between chromophores allow for stronger electronic coupling, while the coordination to the SBU modifies electron delocalization, both of which significantly enhance $\sigma^{(2)}$. This effect is more pronounced than the increased polarization observed in the Sr-based MOF, which was previously thought to be a dominant contributor.^[11f, 11k]

References

- [1] G. I. Stegeman, R. A. Stegeman, *Nonlinear Optics: Phenomena, Materials and Devices*, Wiley, 2012.
- [2] a) G. S. He, L.-S. Tan, Q. Zheng, P. N. Prasad, *Chem. Rev.* 2008, 108, 1245-1330; b) V. Nathan, A. H. Guenther, S. S. Mitra, *J. Opt. Soc. Am. B* 1985, 2, 294-316.
- [3] D. R. Miller, J. W. Jarrett, A. M. Hassan, A. K. Dunn, *Curr. Opin. Biomed. Eng.* 2017, 4, 32-39.
- [4] J. D. Bhawalkar, N. D. Kumar, C.-F. Zhao, P. N. Prasad, *J. Clin. Laser Med. Surg.* 1997, 15, 201-204.
- [5] S. Maruo, O. Nakamura, S. Kawata, *Opt. Lett.* 1997, 22, 132-134.
- [6] L. W. Tutt, T. F. Boggess, *Prog. Quantum Electron.* 1993, 17, 299-338.
- [7] a) J. Bhawalkar, G. He, P. Prasad, *Rep. Prog. Phys.* 1996, 59, 1041; b) F. Zhou, X. Ran, D. Fan, S. Lu, W. Ji, *Adv. Opt. Mater.* 2021, 9, 2100292; c) Y. Wang, V. D. Ta, Y. Gao, T. C. He, R. Chen, E. Mutlugun, H. V. Demir, H. D. Sun, *Adv. Mater.* 2014, 26, 2954-2961.
- [8] a) R. Medishetty, J. K. Zaręba, D. Mayer, M. Samoć, R. A. Fischer, *Chem. Soc. Rev.* 2017, 46, 4976-5004; b) S. J. Weishäupl, D. C. Mayer, Y. Cui, P. Kumar, H. Oberhofer, R. A. Fischer, J. Hauer, A. Pöthig, *J. Mater. Chem. C* 2022, 10, 6912-6934.
- [9] a) D. C. Mayer, A. Manzi, R. Medishetty, B. Winkler, C. Schneider, G. Kieslich, A. Pöthig, J. Feldmann, R. A. Fischer, *J. Am. Chem. Soc.* 2019, 141, 11594-11602; b) N. B. Shustova, B. D. McCarthy, M. Dinca, *J. Am. Chem. Soc.* 2011, 133, 20126-20129; c) R. Haldar, M. Jakoby, M. Kozłowska, M. Rahman Khan, H. Chen, Y. Pramudya, B. S. Richards, L. Heinke, W. Wenzel, *F. Odobel, Chem. – Eur. J.* 2020, 26, 17016-17020.
- [10] A. Kirchon, L. Feng, H. F. Drake, E. A. Joseph, H.-C. Zhou, *Chem. Soc. Rev.* 2018, 47, 8611-8638.
- [11] a) N. Liu, Z. Chen, W. Fan, J. Su, T. Lin, S. Xiao, J. Meng, J. He, J. J. Vittal, J. Jiang, *Angew. Chem. Int. Ed.* 2022, 134, e202115205; b) H. S. Quah, W. Chen, M. K. Schreyer, H. Yang, M. W. Wong, W. Ji, J. J. Vittal, *Nat. Commun.* 2015, 6, 7954; c) B. B. Rath, D. Kottlilil, W. Ji, J. J. Vittal, *ACS Appl. Mater. Interfaces* 2023, 15, 26939-26945; d) R. Medishetty, V. Nalla, L. Nemec, S. Henke, D. Mayer, H. Sun, K. Reuter, R. A. Fischer, *Adv. Mater.* 2017, 29, 1605637; e) R. Medishetty, L. Nemec, V. Nalla, S. Henke, M. Samoć, K. Reuter, R. A. Fischer, *Angew. Chem. Int. Ed.* 2017, 56, 14743-14748; f) S. J. Weishäupl, Y. Cui, S. N. Deger, H. Syed, A. Ovsianikov, J. Hauer, A. Pöthig, R. A. Fischer, *Chem. Mater.* 2022, 34, 7402-7411; g) S. N. Deger, Y. Cui, J. Warnan, R. A. Fischer, F. Šanda, J. Hauer, A. Pöthig, *ACS Appl. Opt. Mater.* 2024, 2, 1770-1779; h) H. S. Quah, V. Nalla, K. Zheng, C. A. Lee, X. Liu, J. J. Vittal, *Chem. Mater.* 2017, 29, 7424-7430; i) H. Yuan, X. Xu, Z. Qiao, D. Kottlilil, D. Shi, W. Fan, Y. D. Yuan, X. Yu, A. Babusenar, M. Zhang, W. Ji, *Adv. Opt. Mater.* 2024, 12, 2302405; j) D. C. Mayer, J. K. Zaręba, G. Raudaschl-Sieber, A. Pöthig, M. Chołuj, R. Zaleśny, M. Samoć, R. A. Fischer, *Chem. Mater.* 2020, 32, 5682-5690; k) S.-C. Wang, Q.-S. Zhang, Z. Wang, L. Zheng, X.-D. Zhang, Y.-N. Fan, P.-Y. Fu, X.-H. Xiong, M. Pan, *Angew. Chem. Int. Ed.* 2022, 61, e202211356. l) S. N. Deger, A. Mauri, Y. Cui, S. J. Weishäupl, A. D. Özdemir, H. Syed, A. Ovsianikov, W. Wenzel, A. Pöthig, J. Hauer, M. Kozłowska, R. A. Fischer, *Adv. Funct. Mater.* 2025, 2424656

Calculations of d-d transition energies of Ni^{2+} in KMgF_3 : effects of structure, pressure and exact exchange.

Alexander Platonenko^a, Mikhail Brik^a, Anatoli I Popov^b, Michal Piasecki^a

^a Jan Długosz University, Armii Krajowej 13/15, Częstochowa, 42-201, POLAND

^b Institute of Solid State Physics, Kengaraga street 8, Riga, LV1063, LATVIA

e-mail: alexander.platonenko@gmail.com

Potassium magnesium fluoride is a widely used host material for optical applications. As wide-gap material ($E_g \sim 12$ eV) it is a perfect compound to accommodate as dopants various transition metal or rare earth metal ions and achieve good luminescent properties. The energy level diagrams and, thus, optical absorption spectra of dopant ions can be assessed with Tanabe-Sugano diagrams, which relies on crystal field strength and surroundings of the ion. Such information can be easily obtained from a ground state DFT calculations. However, there remains a lack of information regarding many aspects of non-ground state d-electron configurations of dopant ions. Previously d-d transition in $\text{NiO}^{1,2}$ were calculated using direct Δ -SCF approach which yielded good agreement with experimental results and providing descriptions of the charge and spin distributions. In this study, we present our results on direct calculations of excited Ni^{2+} states in KMgF_3 matrix using CRYSTAL23 code. Absorption energies were estimated for single-, double-electron excitations, spin-flip excitations ($z^2\uparrow \rightarrow z^2\downarrow$), as well we analyzed the effect of pressure on the excitation energies and effect of exact exchange.

To simulate isolated Ni^{2+} ion in KMgF_3 lattice we use $3\times 3\times 3$ supercell consisting of 135 atoms and substituting one Mg ion with Ni ion, where the ground state of Ni^{2+} ion is $d^8 - t_{2g}^6 e_g^2$. To obtain the electron configuration of the excited state eigenvalues of selected d-orbitals were shifted during SCF cycles. In this case, ground and excited states are calculated identically with the same method and excitation is treated like a local defect in periodic lattice. In this way, all 45 microstates of Ni^{2+} ion can be obtained. Our results are in good agreement with experimentally observed absorption and emission energies; as well correctly reproduce energy shifts under applied hydrostatic pressure. The effect of added percentage of exact exchange to $r^2\text{SCAN}$ XC functional in terms of bond lengths and atomic charges, i.e. resulting crystal field strength, on resulting energies is discussed.

[1] D.S. Middlemiss and W. C. Mackrodt, *Molecular Physics*, **103**, 2513-2525 (2005) First principles study of d \rightarrow d excitations in bulk NiO

[2] W.C. Mackrodt, S. Salustro, B. Civalleri, R. Dovesi, *Journal of Physics: Condensed Matter*, **30**, 495901 (2018) Low energy excitations in NiO based on adirect Δ -SCF approach

Impact of the Protein Environment on the Excited States of the Pigments in Photosynthetic Complexes

Gabrielė Rankelytė,^a Jevgenij Chmeliov,^{a,b} Andrius Gelzinis^{a,b} and Leonas Valkunas^{a,b}

^aCenter for Physical Sciences and Technology, Department of Molecular Compound Physics, Savanorių Ave. 231, Vilnius – LITHUANIA

^bVilnius University, Faculty of Physics, Institute of Chemical Physics, Saulėtekio av. 9, III bld., Vilnius – LITHUANIA

e-mail: gabriele.rankelyte@fmf.lt

The most efficient organisms that carry out photosynthesis are higher plants. Photosystem I (PSI) is the most efficient light-to-energy conversion apparatus where almost all light, absorbed by the light harvesting antenna LHCI, is converted to chemical energy¹. In plants, light harvesting antenna of PSI is composed of four species of LHCI complexes. They all have very similar structure (Fig. 1); however, their spectral properties are different. The excitation dynamics in LHCI are highly affected by the charge-transfer (CT) states that occur between the pigments. Known charge-transfer sites in LHCI do not completely explain the spectral properties of this antenna suggesting the presence of more CT states. The energy of these states is affected by the surrounding environment (pigments and protein). In our work, we investigated the LHCI of PSI complex structure², available at Protein Data Bank (PDB ID: 5L8R). Properties of the excited states of the pigments were calculated using “VU HPC” Saulėtekis supercomputer. Charge-density coupling method³ was used to evaluate excited state energy shifts, caused by the electrostatic environment. The results of the CDC method were compared to the results of QC calculations performed directly in the field of electrostatic charges. Our findings demonstrate the sensitivity of pigment excited state properties to changes in the surrounding environmental geometry (charge placement) and protein protonation pattern.

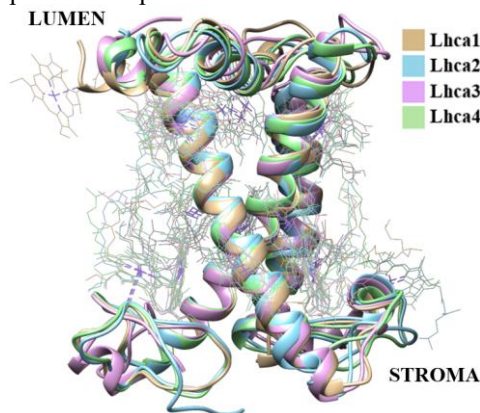


Fig. 1. Matched Lhca1-Lhca4 sub-complexes of LHCI (PDB ID: 5L8R, chains 1-4).

- [1] R. Croce and H. van Amerongen, *Photosynth. Res.*, **116**, 153-166 (2013) Light-harvesting in Photosystem I.
- [2] Y. Mazor, A. Borovikova, I. Caspy and N. Nelson, *Nat. Plants.*, **3**, 17014-17014 (2017) Structure of the Plant Photosystem I Supercomplex at 2.6 Å Resolution.
- [3] T. Renger and F. Müh, *Phys. Chem. Chem. Phys.*, **15**, 3348-3371 (2013) Understanding Photosynthetic Light-harvesting: a Bottom Up Theoretical Approach.

Exploring the Complex Solid-State Landscape of Carbamazepine using Low-Frequency Raman Spectroscopy

Peter III J. G. Remoto,^a Karlis Bērziņš^b, Sara J. Fraser-Miller^c, Timothy M. Korter^d, Thomas Rades^b, Jukka Rantanen^b, and Keith Gordon^a

^aUniversity of Otago, Te Whai Ao - The Dodd-Walls Centre for Photonic and Quantum Technologies, Department of Chemistry, Dunedin – New Zealand

^bUniversity of Copenhagen, Department of Pharmacy, Copenhagen – Denmark

^cFlinders University, College of Science and Engineering, Adelaide – Australia

^dSyracuse University, Center for Science and Technology, Department of Chemistry, Syracuse, New York – United States

e-mail: rempe782@student.otago.ac.nz

Pharmaceutical products must be carefully developed and formulated to ensure that they are consistently safe and of the desired quality for general use. Pharmaceutical products are composed of active pharmaceutical ingredients (APIs) and excipients. Active pharmaceutical ingredients (APIs) can exist in numerous phases, including polymorphs, hydrates/solvates, salts/co-crystals and amorphous phases that lack long-range molecular order and exhibit only certain localized (short-range) structures, if any.

Transformations between the classes and types of solid-state forms is an important property to consider. This is because physicochemical properties such as solubility and dissolution rates differ between solid-state forms. Therefore, detection of such changes is critical for accurate pharmaceutical dosage and drug quality. Different methods can be used to detect such changes which include thermal gravimetric analysis, differential scanning calorimetry, x-ray diffraction, and vibrational techniques like infrared spectroscopy and Raman spectroscopy.

Raman spectroscopy offers rapid, non-destructive, and relatively inexpensive measurements for structural characterisation. Advancements in optics and filter technology have made low-energy Raman scattering more accessible. In the low-frequency Raman (LFR) region, lattice vibrational modes (so-called phonon or intermolecular vibrational modes) can be detected. Whereas mid-frequency Raman (MFR) region typically presents intramolecular vibrational modes. Previous studies have shown that LFR and MFR regions offer unique advantages to monitor solid-state transformations.^{1,2} Carbamazepine displays quite a complex solid-state landscape with its five known anhydrous forms (CBZ-I, CBZ-II, CBZ-III, CBZ-IV, and CBZ-V) and one hydrate form (carbamazepine dihydrate). Each solid-state form has different hydrogen bonding patterns. In this study, these solid-state forms were characterized using their low- and mid-frequency Raman spectra. In addition, investigate the dehydration behaviour of carbamazepine dihydrate. Experimental data were supported and assigned using DFT calculations with periodic boundary conditions.

[1] Remoto, P. J. G., Berzins, K., Miller, S. J., Korter, T., Rades, T., Rantanen, J., and Gordon, K. C. *Cryst. Growth Des.*, **15**, 4579-4583 (2023). Elucidating the Dehydration Mechanism of Nitrofurantoin Monohydrate II Using Low-Frequency Raman Spectroscopy.

[2] Robert, C., Fraser-Miller, S. J., Bērziņš, K., Okeyo, P. O., Rantanen, J., Rades, T., and Gordon, K. C. *Mol. Pharm.*, **18**, 1264-1276 (2021). Monitoring the Isothermal Dehydration of Crystalline Hydrates Using Low-Frequency Raman Spectroscopy.

From Hybrid-DFT to Million-Atom MD: Accurate and Scalable qSNAP Potential for Radiation Damage in BaF₂

Rostislavs Rostovskis,^a Aleksandrs Platonenko^b and Anatoli Popov^a

^a*Institute of Solid State Physics, University of Latvia, 8 Kengaraga Str., Lv-1063 Riga, Latvia*

^b*Jan Długosz University, Armii Krajowej 13/15, Częstochowa, 42-201, Poland*

rostislavs.rostovskis@cfi.lu.lv

We present a machine-learning interatomic potential (MLIP) study of radiation-induced defect cascades in barium fluoride (BaF₂), employing the q-Spectral Neighbor Analysis Potential (qSNAP) framework. qSNAP extends the Spectral Neighbor Analysis Potential (SNAP)¹ by including quadratic contributions of the bispectrum descriptors, thereby enhancing the potential's expressiveness, as introduced in the original qSNAP publication². Our MLIP is a hybrid model comprising three components: a long-range Coulomb interaction handled via the PPPM solver in LAMMPS, a short-range qSNAP term, and a Ziegler–Biersack–Littmark (ZBL) repulsive correction at very short interatomic separations. The qSNAP parameters were generated “on-the-fly” by iteratively enriching the training set with high-energy configurations sampled during molecular dynamics (MD) in LAMMPS, using structures ranging from 12 to 96 atoms to ensure both computational efficiency and diversity of local environments. Reference data were obtained from hybrid-functional DFT (HSEsol) calculations carried out with the CRYSTAL23 code. During on-the-fly training, forces, energies, and stress tensors predicted by the MLIP for newly sampled structures consistently matched those computed via DFT, confirming the potential's reliability across diverse configurations.

To investigate cascade formation, we performed MD cascade simulations in LAMMPS by assigning a range of kinetic energies to a primary knock-on atom (PKA) along multiple crystal directions. The simulation cell was partitioned into a thermostatted boundary region (NVT) and an unconstrained core (NVE), allowing the cascade to evolve and the system to cool naturally. After relaxation, defect populations were analyzed to identify intrinsic defects. Given BaF₂'s role as a widely used scintillator material, such large-scale MD - enabled by our MLIP to handle hundreds of thousands to millions of atoms - is critical for predictive modeling of defect formation and evolution under irradiation. Moreover, in MD simulations of systems containing hundreds of thousands of atoms, each timestep required only a few seconds of wall time on a single central processor, underscoring the method's computational efficiency.

[1] A. P. Thompson, L. P. Swiler, C. R. Trott, S. M. Foiles and G. J. Tucker, J. Comput. Phys., 285, 316–330 (2015) Spectral Neighbor Analysis Method for Automated Generation of Quantum-Accurate Interatomic Potentials

[2] M. A. Wood and A. Thompson, J. Chem. Phys., 148, 241721 (2018) Extending the accuracy of the SNAP interatomic potential form

Control Of Chemical Bonds And Motif Stereochemistry On Magnetic Superexchange In Coordination Network Based Spintronics

Sounak Sarkar,^a Piero Macchi^a

^aDepartment of Chemistry, Materials and Chemical Engineering, Politecnico di Milano, Via Mancinelli 7, 20131, Milano, Italy

e-mail: presenting. sounak.sarkar@polimi.it

Coordination polymers (CP) offer a wide compositional space in terms of metals and ligands to design a network with desired magnetic (ferromagnetic/antiferromagnetic) ordering¹ as compared to inorganic spintronics with limited chemical tunability. The periodic arrangement of paramagnetic metal centres in these framework crystal structures enables cooperative exchange interactions between them through the organic linkers resulting in long-range magnetic order along one or more directions. Currently, an active focus of research in magnetic CPs involves increasing the strength of magnetic exchange between spin centres to realize the implementation of these magnetic materials in practical applications. In this context, the role of ligands in promoting magnetic exchange interactions in solid-state needs to be thoroughly studied. In this study, we selected a pair of antiferromagnetic ‘quasi-isostructural’ CPs- Cu(HCOO)₄(pyrazine)₂ (CuFmPyz)² and Cu(HCOO)₄(pyrimidine)₂ (CuFmPym)³ whose exchange coupling constant (J) differs by an order of magnitude (Figure 1). The characteristic topology comprising of Cu and formate ions along two directions in individual CP is similar. Nevertheless, in the third dimension, the stereochemistry of Cu-ligand-Cu motif is linear in CuFmPyz, $\tau = 180^\circ$ while in CuFmPym, the corresponding motif is V-shaped or bent, $\tau = 117^\circ$. To study the control of metal–ligand bonds and motif stereochemistry on superexchange mechanism in respective CPs, we executed accurate modelling of electron density (ED) against high-quality, high-resolution ($d \leq 0.4 \text{ \AA}$) X-ray diffraction data measured using Ag source at 100 K. Comparative bonding analysis of these ED models was further conducted to identify the nature of possible superexchange pathways in respective CPs. We believe the outcomes from this study will help us to establish a robust correlation between metal–ligand bonding and strength of magnetic exchange coupling and subsequently will aid the material research community to design new spintronic CPs.

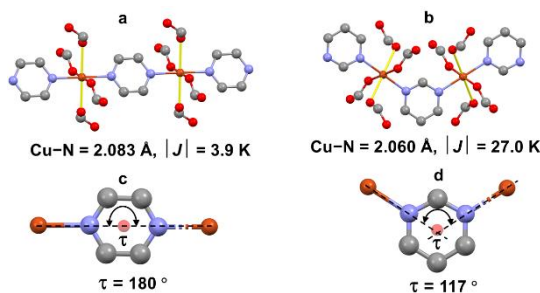


Figure 1: Single chain formed by Cu and respective bridging ligand in the crystal structure of a) CuFmPyz and b) CuFmPym. Yellow Cu–O bonds indicate the Jahn-Teller axis. $|J|$ is the magnitude of exchange coupling constant derived from magnetic measurement. Building unit of the single chain with framework angle τ in c) CuFmPyz and d) CuFmPym. Cu (brown), O (red), C (grey), N (blue).

[1] A. E. Thorarinsdottir et al., *Chem. Rev.* **120** (2020) 8716.

[2] J. L. Manson et al., *Dalton Trans.*, **2003**, 2905.

[3] J. L. Manson et al., *Inorg. Chem.* **44** (2005) 989.

Quantum chemical investigation of multi-redox states in organic conjugated redox ladder type polymers for electrochemical energy storage systems

Shuailong Wang,¹ Daniele Fazzi¹ and Fabrizia Negri¹

¹Department of Chemistry "Giacomo Ciamician", University of Bologna, via F. Selmi 2, 40126 Bologna (Italy)

e-mail: shuailong.wang@studio.unibo.it

Electrochemical energy storage (EES) devices, such as batteries and supercapacitors, play a vital role in our modern society.¹ The request of materials able to store and release electrical energy at demand is continuously growing, challenging the actual state of the art of EES technologies. Lithium-ion batteries (LIB), as composed by inorganic electrode materials (e.g., nickel-cobalt alloys), have been largely investigated and used, however, they present limits related to their environmental sustainability and low charge capacity.

Organic conjugated redox polymers (OCRP) can be considered an effective alternative to inorganic-based EES materials, being environmentally friendly, and easy to design and fabricate.² However, little is known about their fundamental structure vs. redox-property relationships.

In this contribution, we investigate via quantum-chemical calculations the structural and electronic properties of a special class of OCRPs, namely ladder polymers.³ They are characterized by a rigid and highly conjugated backbone, leading to semi-crystalline solid-state morphologies featuring high charge and ion mobilities. The ladder OCRPs we considered are polyquinoxalines (PQL) and SBBL, the latter being a simplified derivative of benzobisimidazobenzophenanthroline (BBL), a well-known polymer with high charge, thermal and ion mobility.^{4,5}

By combining density functional theory (DFT), broken-symmetry DFT (BS-DFT) and fragment orbital density analysis (FOD) we revealed the poly-radicaloid character of the electronic structure of neutral and multi-redox states.⁶ We found that negative (electron) and positive (hole) charges, here defined polarons, relax on localized states of the polymer chain, thus featuring different structural relaxations and electron-phonon coupling properties. Multi-charged species, revealed complex electronic structures, as characterized by quasi-degenerate multiply states showing various spin multiplicities (e.g., doublet, triplet, quartet, quintet, etc.) and response properties. To validate the conclusion reliability, various functions are utilized for comparison in electronic properties, thus better reflecting the function choice.

To model realistic operating functions, the interaction mechanisms between the conjugated redox centers and multiple metal-cations beyond lithium (e.g., Na⁺ and K⁺) are investigated, thus comprehensively elucidating the ions insertion/desertion processes occurring upon the electrochemical event. Computational study aims at introducing an appropriate of the electronic structure and redox properties of ORCPs for organic electrodes.

[1] J.-M. Tarascon and M. Armand, *Nature* **2001**, 414, 359-367. Issues and challenges facing rechargeable lithium batteries.

[2] J. Xie, P. Gu, Q. Zhang, *ACS Energy Lett.* **2017**, 2, 1985-1996. Nanostructured conjugated polymers: toward highperformance organic electrodes for rechargeable batteries.

[3] J. Lee et al., *Chem. Sci.* **2017**, 8, 2503-2521. Fully conjugated ladder polymers.

[4] S. Wang et al., *Adv. Mater.* **2016**, 28, 10764-10771. Thermoelectric properties of solution-processed n-doped ladder-type conducting polymers.

[5] D. Fazzi and F. Negri, *Adv. Electron. Mater.* **2021**, 7, 2000786. Addressing the elusive polaronic nature of multiple redox states in a π -conjugated ladder-type polymer.

[6] D. Fazzi et al., *J. Mater. Chem. C* **2019**, 7, 12876-12885. Polarons in π -conjugated ladder-type polymers: a broken symmetry density functional description.

DFT Modeling Data Curation for Machine Learning Applications

Alina Zhidkovskaya,^a Evgeny Blokhin^a

^a*Materials Platform for Data Science LLC, Sepapaja 6, Tallinn – ESTONIA*

e-mail: alina@mpds.io

We present an integrated computational framework for high-throughput materials discovery, combining first-principles simulations, data curation, and machine learning (ML). Our workflow begins with theoretical simulations based on experimentally validated crystal structures from the Materials Platform for Data Science (MPDS). We perform automated high-throughput computations using two complementary engines:

- CRYSTAL for ab initio quantum-chemical calculations (electronic structure, thermodynamics, spectroscopy),
- FLEUR as a complementary simulation engine implementing full-electron linearized augmented-plane-wave method.

The primary goal is to generate high-fidelity, curated datasets of nanoscale material properties.

In addition to data collection, we train models to predict chemical properties based on the molecular structure of a substance.

Extended structure descriptors include:

- Compositional features (atom types, their number, ordinal numbers),
- Graph-based representations encoding atomic connectivity for graph neural networks (GNN, GAT).

We employ a variety of algorithms:

- Ensemble methods (Random Forests, Gradient Boosting) for interpretability,
- Deep learning (GNNs, Transformers) for capturing complex structure-property relationships.

Some of the properties we have worked on predicting include the Seebeck coefficient and thermal conductivity.

An automated data preparation pipeline is currently under development, laying the foundation for scalable and fully reproducible ML workflows in materials science.